Channel-Arc Model of DC Hydrogen Arc Plasma: Influence Of Radiation and Very High Pressure

Papa Gueye, Yann Cressault, Vandad-Julien Rohani, Laurent Fulcheri

CHANNEL-ARC MODEL OF DC HYDROGEN ARC PLASMA: INFLUENCE OF RADIATION AND VERY HIGH PRESSURE

P. Gueye [1], Y. Cressault[2], V. Rohani[1] and L. Fulcheri[1]

[1] *MINES ParisTech, PSL-Research University, PERSEE Centre procédés, énergies renouvelables et systèmes énergétiques, CS 10207 rue Claude Daunesse 06904 Sophia Antipolis Cedex, France*

Tel: +33.493.957.540, Email: papa.gueye@mines-paristech.fr

[2] *Université de Toulouse, UPS, INPT, LAPLACE (Laboratoire Plasma et Conversion d'Energie), 118 route de Narbonne, F-31062 Toulouse Cedex 9, France*

Tel: +33.561.558.221, Email: cressault@laplace.univ-tlse.fr

Abstract: This study focuses on a wall-stabilized hydrogen arc column at low current. The problem is solved numerically by using simplified Ohm's law and deriving the stationary Elenbaas-Heller equation from an energy balance where conduction and radiation are considered. The latter is computed using Lowke's approach of net emission coefficient where both background continuum and line spectrum are considered. This work aims to derive the electric characteristic and its sensibility to the model parameters and study the influence of a 20-bar pressure.

Keywords: radiation, hydrogen plasma, high pressure, channel arc model

Introduction

PERSEE group has been working on the plasma-assisted conversion of hydrocarbons. This led to the development of a three-phase plasma torch which attained pre-industrial size and runs at atmospheric pressure with different pure and mixture gases (argon, helium, nitrogen, air…) [1-3]. Studies are also conducted for its improvement toward a high and very high operational pressure with pure hydrogen. While advanced computational methods as CFD, MHD are costly, there are simplified models such as channel arc models that give crucial results and have proven to compare well with experiments [4-5].

1. General assumptions

At the outset it should be mentioned that the theory of the arc as developed here entirely disregards any phenomena that are due to the presence of electrodes.
Hence we consider here the positive column voltage much bigger than cathode and anode falls and, as for most situations, this column part of the discharge determines the operational characteristics of the arc. In plasmas using inert gases like argon, the electron-neutral energy exchange is less effective and requires high currents and electron densities to reach quasi equilibrium whereas in molecular gases such as hydrogen, the validity of the local thermodynamic equilibrium can be assumed at any current, thanks to sufficient electronic densities and moderated temperature and density gradients for small diffusive fluxes [6].

2. Arc modeling

One of the major issues to be dealt with arc plasma is its stability. The easiest solution is to surround the arc with a well-cooled wall that should be able to absorb the energy losses without being destroyed.
Several investigators have studied the problem of the approach to the asymptotic column. One of the most striking formulations for tube arc problems is that of Stine [5] showing particularly good agreement with experiment. Thus we consider here positive column arc plasma burning inside a cylindrical tube whose walls are maintained at a constant temperature. However, the stronger the confinement, the larger the gradients in the plasma arc. We assume nevertheless that the local thermodynamic equilibrium remains valid in spite of such confinement. This can be justified a posteriori with relatively low densities and temperature gradients, inducing then small diffusive fluxes.

3. Equations

In order to provide a reasonable description of the manner in which the DC arc behaves, it is necessary to derive the differential equation that describes the energy-transfer processes within the arc column. The temperature distribution in a long cylindrical steady-state thermal plasma column stabilized by walls in a tube of radius R is described by the well-known Elenbaas-Heller equation which we derive in the following sections.

3 .1. Electric field

For the steady-state arc, the Faraday's law in cylindrical coordinates gives

$$\nabla \times \vec{E} = \vec{0} \tag{3}$$

$$\nabla \times \vec{E} = \left(\frac{1}{r}\frac{\partial E_z}{\partial \theta} - \frac{\partial E_\theta}{\partial z}\right)\vec{e_r} + \left(\frac{\partial E_r}{\partial z} - \frac{\partial E_z}{\partial r}\right)\vec{e_\theta} + \left(\frac{1}{r}\frac{\partial (rE_\theta)}{\partial r} - \frac{1}{r}\frac{\partial E_r}{\partial \theta}\right)\vec{e_z}$$

The component E_θ is null for a symmetry matter. Moreover, the arc column refers to that part of the arc plasma that is axially invariant. Thus we finally have

$$\frac{\partial E_z}{\partial r} = 0 \tag{4}$$

Across the cross section of the positive column, the electric field is constant and defines the voltage.

3.2. Elenbaas-Heller equation

The DC positive column energy equation is given by

$$div\left[q + pv_0 + \rho v_0 (u + \frac{v_0^{\ 2}}{2}) \right] - jE + q_{rad} = 0 \quad (5)$$

Within the low current considered here, the cathode jet due to Maecker's effect [7] is negligible, so is the self-magnetic field. Thus any convective contribution of the Lorentz force in the energy balance vanishes. Plus, as the arc is not blown, it is justified to set the mean gas velocity v_0 to zero. Due to the absence of magnetic field, either external or self-magnetic field, the generalized Ohm's law can be simply written as

$$\vec{j} = \sigma \vec{E} \qquad (7)$$

The term of radiation is computed using Lowke's approach of the net emission coefficient [8]. Details will be provided in the next section. The radiated power per unit volume is thus given by

$$q_{rad} = 4\pi\varepsilon_N \qquad (8)$$

Assuming heat transfer by conduction with the Fourier law

$$q = -\lambda \nabla T \qquad (9)$$

We finally obtain the energy balance of the steady-state column in cylindrical coordinates as

$$\sigma E^2 + \frac{1}{r}\frac{d}{dr}(r\kappa \frac{dT}{dr}) - 4\pi\varepsilon_N = 0 \qquad (11)$$

This equation is known as the Elenbaas-Heller equation. Boundary conditions for (9) are $dT / dr = 0$ at r=0, and $T = T_w$ at r=R. The electric control parameter here is the electric field rather than the current for sake of simplicity. The current is then derived from E by

$$I = 2\pi E \int_0^R \sigma(T) r dr \qquad (12)$$

The Elenbaas-Heller equation together with relation [12] permits calculations of the function $E(I)$, which is the current-voltage characteristic of the plasma column determined by the following material functions: electric conductivity $\sigma(T)$ and thermal conductivity $\kappa(T)$. These are computed from the software T&T Winner [9] with a temperature from 300 K to 20 000 K.

3.3. Net emission coefficient

In most plasma studies, radiation is neglected or estimated with empirical formulas [6]. However, at high current and pressure, the heat transfer is mostly related with radiation [10]. For higher accuracy, there is then need to consider the latter in the mathematical formulation.

To calculate the net emission coefficient, which is the power radiated per unit volume and unit solid angle, we must solve the equation of radiative transfer which is written in the form [8]

$$\varepsilon_{N_\nu} = k'_\nu (B_\nu - J_\nu) \qquad (13)$$

where

$$k'_\nu = k_\nu \left[1 - \exp(-\frac{h\nu}{kT}) \right] \qquad (14)$$

$$B_\nu = \frac{2h\nu^3}{c^2}\left[\exp(\frac{h\nu}{kT}) - 1 \right]^{-1} \qquad (15)$$

$$J_\nu = \frac{1}{4\pi}\int_{4\pi} I_\nu(\mathbf{r},\mathbf{n}) d\Omega \qquad (16)$$

k'_ν is the absorption coefficient corrected for induced emission and k_ν is the normal absorption coefficient ; B_ν is the black body radiation intensity ; J_ν is the average radiation intensity; I_ν is the radiation intensity in the $\mathbf{r}$ direction, through a surface unit of normal direction $\mathbf{n}$.

Lowke and Liebermann [11] solved this radiative problem for two geometries and show that one can replace, as a first approximation and with 90% of accuracy, an isothermal cylinder by an isothermal sphere. In these conditions, one has:

$$\varepsilon_N = \int_0^\infty k'_\nu B_\nu \exp(-k'_\nu R) d\nu \qquad (17)$$

To derive the net emission coefficient, it is thus necessary to compute first the absorption coefficient corrected for induced emission. This was derived from the recent work of T. Billoux [12] where both background continuum and line spectrum were considered. This gives a database with a temperature range from 300 to 30.000 K with wavelengths from 0.209 µm to infrared and considers the radiation from back continuum, either molecular (H2) or atomic (H2), and 74 lines spectrum for hydrogen.

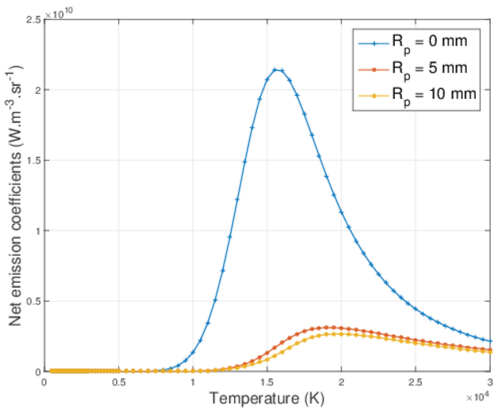

Fig. 1: Net emission coefficient of hydrogen plasma with temperature at 1 bar and for different plasma radii.

The plasma thickness is considered for the derivation of net emission coefficient, as self-absorption should be taken into account. ε_N corresponds to the difference between the local emitted radiation and that emitted somewhere else and absorbed locally. ε_N decreases then when the plasma radius increases as shown in figure 1.

4. Results

4.1. Temperature profiles

With a MATLAB code, we derive the temperature profile for a given electric field and pressure. The difficult part of the calculation was to enforce the boundary condition at the wall because the latter is in fact a strong function of the core temperature. Once a self-consistent solution is reached, we can generate a family of temperature profiles presented in figure 2. It can be deduced from it that the core temperature increases with the current. This agrees with what one might expect intuitively. Plus, at high current and temperatures, the profile becomes much squarer as the radiation losses begin to dominate. Then we go from a core profile with high gradient to a coreless form.

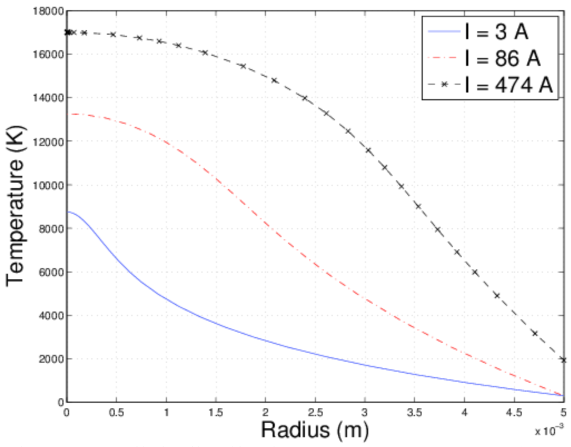

Fig. 2: Radial distribution of temperature of a wall stabilized arc column of 5 mm radius at 1 bar and considering 5 mm plasma radius.

The change in shape of the curves can be interpreted going back to the Elenbaas-Heller equation, with a changing mechanism of heat loss. The primary information on the nature of the radial distribution of temperature follows from the differential equation of energy at the axis:

$$-2\kappa\frac{d^2T}{dr^2}\Big|_{r=0} = \sigma_0 E^2 - q_{rad_0} \tag{18}$$

where $\sigma_0 = \sigma(T_0)$, $q_{rad_0} = q_{rad}(T_0)$. It may be seen that the sign of the equation $\sigma_0 E^2 - q_{rad_0}$ determines the sign of the second derivative of the temperature, i.e. the sign of the curvature of the profile in the immediate vicinity of the arc axis. The assumption of the maximum temperature at the axis of the arc indicates that the strength of the electrical field should satisfy the condition

$$E^2 > q_{rad_0}/\sigma_0 \tag{19}$$

The form of the profile T(r) depends strongly on the nature of variation of the complex q_{rad}/σ with temperature [8]. At low temperature, this is low due to small radiation losses and the temperature profile must have a large enough gradient to drive the conductive loss. It consists then of a narrow central core with a sharp decrease of temperature, i.e. the constricted type arc. This low temperature profiles found here are similar in shape to those derived by Maecker [13] who modeled electric conductivity $\sigma(T)$ as a piecewise linear function of the integrated thermal conductivity $S = \int \kappa dT$ and the solved the non-radiative profile analytically. At high temperature, q_{rad}/σ is great and sufficient heat can be radiated without a large temperature gradient. In this way, as the core temperature increases, the profile becomes flatter in the center and squarer in shape.

Finally, let us notice that a little change of the core temperature can lead to a swing with a temperature increasing radially (that is a heat input is required from the outside) due to the strong temperature dependence of the radiative losses, especially at 20 bars where equation [19] induces to consider absolutely auto-absorption to avoid this swing and have a physical solution.

4.2. Current-voltage characteristic of a hydrogen arc column and pressure

The temperature profile being derived, the current calculation from Ohm's law equation [10] is a straightforward integration. It follows the electric characteristic.

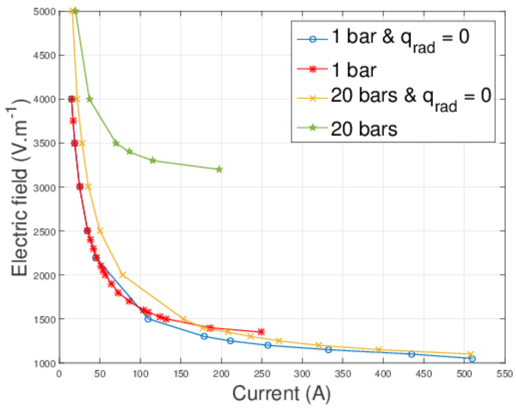

Fig. 3: Current-voltage characteristic of a wall stabilized arc column of 10 mm radius

It comes out from figure 3 that the electric field is decreasing with current. The hyperbolic form of the plots shows that the power per unit length $w = EI$ is almost constant in the current range considered here.

At 1 bar pressure, radiation can be negligible until a current of the order of one hundred amperes whereas at 20 bars, it becomes preponderant even at very low current. Regarding the arc temperature, the figure 4 shows that it decreases with radiation, especially at 20 bars. Such tendency is more and more dire as the pressure is increased.

These remarks on the pressure issue were independent of the tube radius as the latter was varied in a range from 5 to 10 mm. In fact, reducing the confinement was only responsible of a decrease in the electric field at a given current, due to the conjunction of the arc cooling and a modification in temperature profiles, going from an arc flatter at the center to a constricted type arc (see figures 5 through 7).

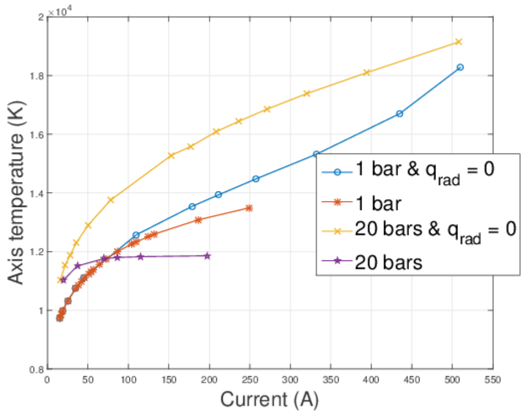

Fig. 4: Temperature at the axis vs current for a wall stabilized arc column of 10 mm radius

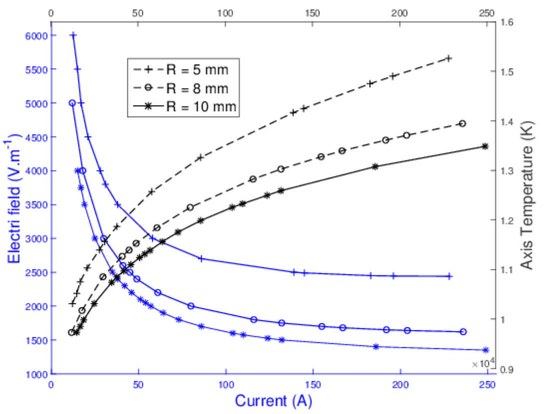

Fig. 5: Electric field and temperature at the axis vs current for a wall stabilized arc column at 1 bar pressure

To summarize the pressure issue, it comes out that changing operational conditions from 1 to 20 bars leads to an electric field multiplied by a factor 2. This is a good agreement with the order of magnitude found from empirical laws in the literature for the effect of pressure on hydrogen blown arcs [14-15]

$$E \propto P^{0.4} \text{ [14]} \quad (20)$$

$$E = A\ln(P) + B \text{ [15]} \quad (21)$$

and for which the multiplying factor is around 3.

Conclusion

This simple wall stabilized hydrogen arc column model gives results that are in line with works on hydrogen current-voltage characteristic [13-15] and on the effect of pressure [14-15]. Moreover, it corroborates the fact that, in high-temperature plasma due to current and/or pressure increase, the radiation constitutes an important energy loss term that must be taken into account in any model.

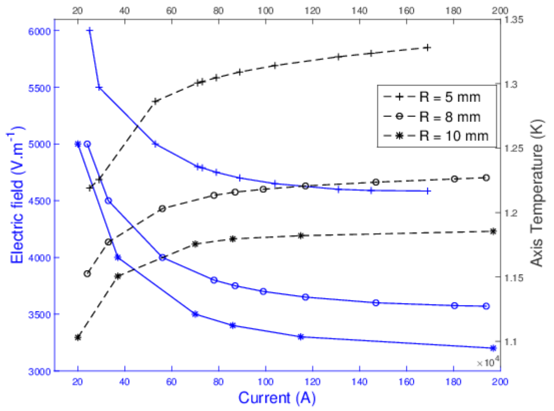

Fig. 6: Electric field and temperature at the axis vs current for a wall stabilized arc column at 20 bar pressure

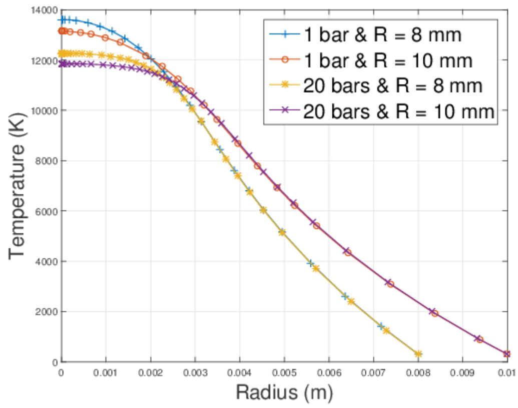

Fig. 7: Radial distribution of temperature of a wall stabilized arc column for different radii, I=195A and at 1 bar and 20 bar pressures.

References

[1] Fulcheri, L. et al, Plasma processing: a step towards the production of new grades of carbon black, Carbon, 40 (2002) 169-176.

[2] Fabry, F., Flamant, G. and Fulcheri, L., Carbon black processing by thermal plasma. Analysis of the particle formation mechanism, Chemical Engineering Science, 56 (2001) 2123-2132.

[3] Rehmet, C., Étude théorique et expérimentale d'une torche plasma triphasée à arcs libres associée à un procédé de gazéification de matière organique, PhD thesis (2013).

[4] Larsen, H. L., AC electric arc models for a laboratory set-up and a silicon metal furnace, PhD (1996).

[5] Stine, H.A, and Watson, V.R, The theoritical enthalpy distribution of air in steady flow along the axis of a direct current, NASA Technical Note D-1331, (1962).

[6] Granovsky, V.L., Electric current in gas, Nauka, Moscow (1971).

[7] Maecker, H., "Plasmaströmungen in Lichtbögen infolge Eigenmagnetische Kompression", Zeitschrift für Physik, Volume 141, , pp. 198-216 (1955)

[8] Lowke, J.J, J. Appl. Phys. **41** 2588 (1970).

[9] B. Pateyron, T&Twinner, Université de Limoges (2009).

[10] B. Pateyron, Contribution à la réalisation et à la modélisation de réacteurs plasmas soufflés ou transférés appliqués à la métallurgie extractive et à la production de poudres ultrafines métalliques ou céramiques (1987).

[11] Lieberman, R.W and Lowke, J.J, J. Quant. Spectrosc. Radiat. Transfer **9** 207 (1969)
[12] T. Billoux, Élaboration d'une base de données radiatives pour des plasmas de type CwHxOyNz et application au transfert radiatif pour des mélanges air, CO2 et CO-H2, in, pp. 1 vol. (226 p.). (2013)
[13] Maecker, Zeitschrift für Physik, Volume 157 (1959).
[14] M F. Zhukov, Thermal plasma torches, CISP, pp.230-241 (1975)
[15] R. Philips et al, Three-phase ac arc heater, ARL 64-29, Aerospace Research Laboratories, US Air Force (1964).